

Ferromagnetic Nanowires with Superconducting Electrodes

V. T. Petrashov, I. A. Sosnin, I. Cox, A. Parsons, C. Troadec

*Department of Physics, Royal Holloway, University of London, Egham, Surrey,
TW20 0EX, U.K.*

The proximity effect in mesoscopic ferromagnet/superconductor (FS) Ni/Al structures of various geometries was studied experimentally on both F- and S-sides of the structures. Samples with a wide range of interface transparency were fabricated. The dependence of the effect on FS interface transparency was investigated. The amplitude of this effect was found to be larger than expected from classical theory of proximity effect. Preliminary experiments showed no phase-sensitive oscillations in Andreev interferometer geometry. Various theoretical models are discussed.

PACS numbers:74.50.+r, 74.80. Fp, 85.30. St.

1. INTRODUCTION

Electronic devices exploiting the spin of conduction electrons rather than their charge have been proposed recently as an alternative to conventional electronics (see e.g. Ref. 1 and references therein). Ferromagnetic materials, being a natural source of spin-polarized electrons for such devices, are in focus of intensive experimental and theoretical investigations. Hybrid ferromagnet/superconductor (FS) structures are prospective candidates for device application and can be useful tools for studying properties of nanometer-size ferromagnets. Recently the measurements of the spin polarization of direct current have been reported for ballistic point contacts.^{2,3} These experiments were in reasonable agreement with both the band structure of ferromagnets⁴ and the general picture of Andreev reflection on the FS interface.⁵ In contrast, recent experiments on diffusive FS nanostructures showed a dramatic disagreement between the theory and the data.

While the theory⁶ predicts any superconducting correlation to decay in the diffusive ferromagnet over the distance $\xi_F = \sqrt{\frac{\hbar D}{k_B T_C}}$ governed by the exchange energy of the ferromagnet, which is of the order of $k_B T_C$ (T_C is the Curie temperature, D , the diffusion constant of the ferromagnet), the experimental results suggest that the influence of the superconductor penetrates into the ferromagnet over a distance up to 10^2 times larger than ξ_F .^{7,9,10}

Here we report further experimental studies of mesoscopic *FS* structures of various geometries. We find that the conductance changes can be of both negative and positive sign at the superconducting transition, with the amplitude of the changes up to 10^2 times larger than theoretical values. We demonstrate that the sign and the amplitude of the effect depend strongly on the interface transparency. Our preliminary experiments with *FS* interferometers showed no phase-periodic oscillations down to the level of $0.1 e^2/h$.

2. EXPERIMENTAL

The samples were fabricated using multiple e-beam lithography. Ni/Al structures were thermally evaporated in a vacuum of 10^{-6} mbar onto a silicon

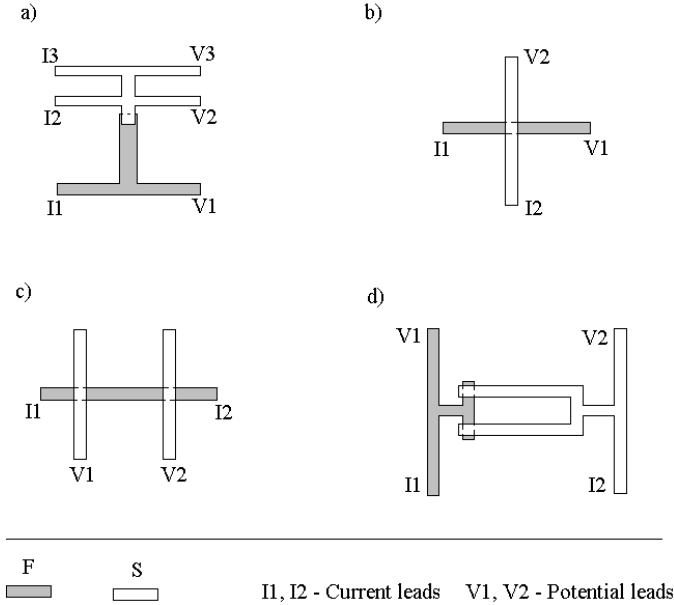


Fig. 1. Sample geometries

Ferromagnetic Nanowires with Superconducting Electrodes

substrate kept at room temperature. The first layer was a ferromagnet (Ni) 40nm thick, the second layer, a superconductor (Al) 60 nm. Various geometries studied are shown in Fig. 1. The resistivities of the films varied from sample to sample and were in the range of 10 - 50 $\mu\Omega$ cm for Ni and 1.0 - 1.5 $\mu\Omega$ cm for Al.

The resistance of the structures was measured by the four-terminal method. Current and potential leads are marked I and V in Fig. 1. The resistance of the structures was measured using both dc and ac signals in the temperature range from 0.27K up to 50K and in magnetic fields up to 5T.

Special care was taken to create interfaces of controllable quality. Before the deposition of the second layer, the contact area was Ar^+ plasma etched. By varying etching parameters, we obtained interfaces of a wide range of transparencies. Wide checking layers were analyzed by Secondary Ion Mass-Spectroscopy (SIMS) with the primary beam of Cs^+ ions. For the best samples, the concentrations of oxygen and carbon at the Ni/Al interface were in the range of 0.1-0.01 of a single atomic layer.

3. RESULTS

Figures 2 a and b show magnetoresistance of the FS junction of sample #1 (geometry of Fig. 1a) measured using contacts ($I1, I2, V1, V2$) at temperatures well above ($T=1.3\text{K}$) and below ($T=0.27\text{K}$) the superconducting transition. At $T=1.3\text{K}$ the junction shows anisotropy magnetoresistance with hysteresis typical for ferromagnetic conductors. At temperatures below the transition, the magnetic field dependence changes drastically. A resistance drop is observed at the superconducting transition of Al in the magnetic field. The amplitude of the drop is close to that observed in the temperature dependence.¹⁰ The hysterisial behaviour is also observed below the superconducting transition.

Some samples showed negative magnetoresistance at small magnetic fields (Fig. 2c). There is a correlation of this feature with the critical current of the superconducting transition of the adjacent superconducting structure ($I2, I3, V2, V3$) presented in Fig. 3d. Note that the critical current for sample #2 goes nearly to zero at small magnetic fields, while that for the sample #1 stays relatively large (about $20\mu\text{A}$). The critical temperature of the superconducting transition of the structure measured using $I2, I3, V2, V3$ at zero magnetic field was within the range 1.0 - 1.05 K for all samples of this geometry.

To study properties of the FS interface itself we used a cross geometry shown in Fig. 1b. In Fig. 3 we show differential voltage-current character-

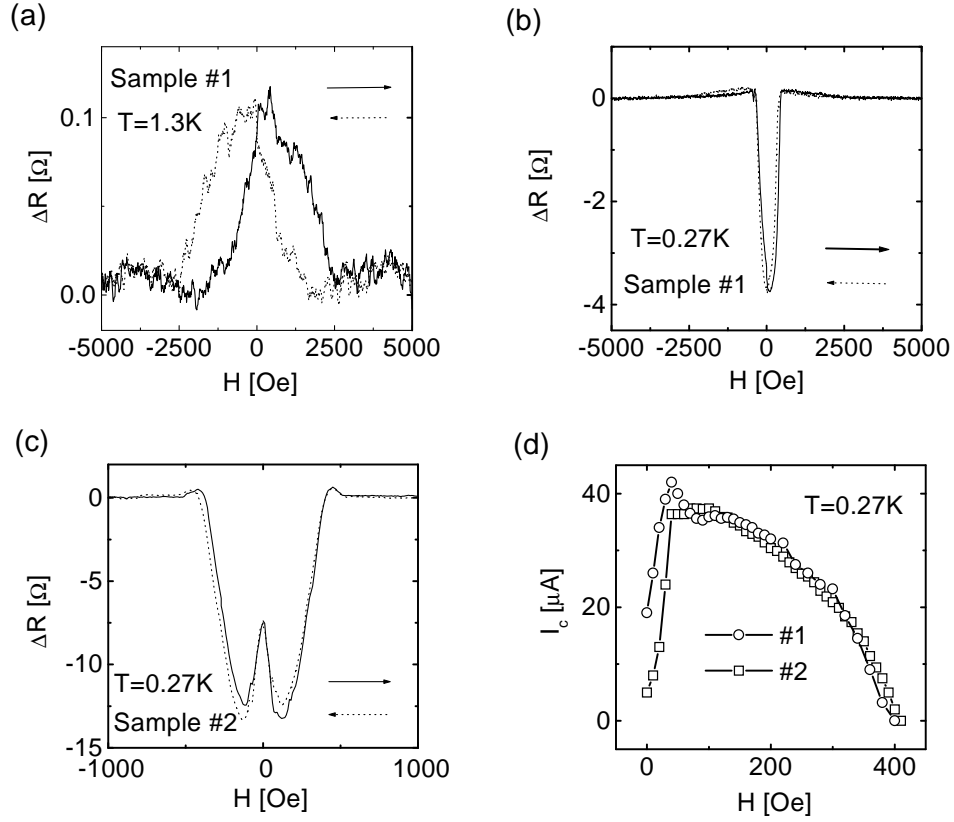


Fig. 2. Magnetoresistance of two samples in geometry Fig. 1a. a) Sample #1 (I_1, I_2, V_1, V_2) above the superconducting transition at $T=1.3\text{K}$ b) Sample #1 (I_1, I_2, V_1, V_2) below the transition at $T=0.27\text{K}$. c) Sample #2 (I_1, I_2, V_1, V_2) at $T=0.27\text{K}$. d) Critical current of the superconducting transition of adjacent superconductor structure (I_2, I_3, V_2, V_3) for samples #1 and #2.

Ferromagnetic Nanowires with Superconducting Electrodes

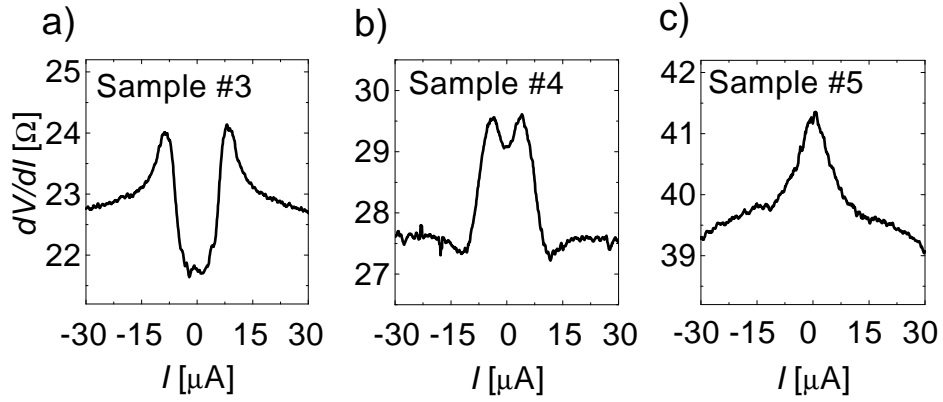


Fig. 3. Differential voltage-current characteristics of three different samples in geometry of Fig. 1b. a) Sample #3, $R_b=22.5\Omega$; b) Sample #4, $R_b=28\Omega$; c) Sample #5, $R_b=39\Omega$.

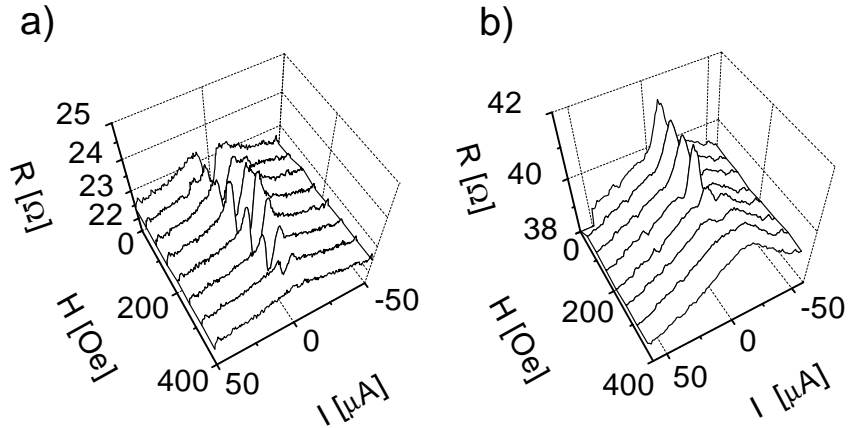


Fig. 4. Applied current - magnetic field 3D-diagrams for samples #3 (a) and #5 (b).

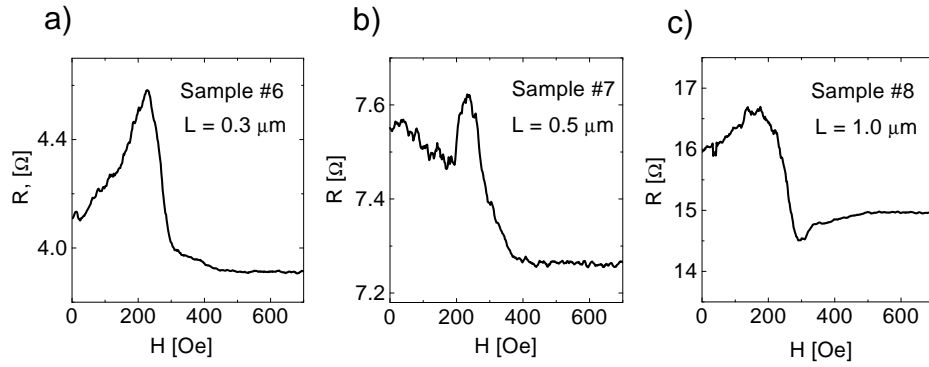


Fig. 5. Magnetoresistance of samples #6-8 in geometry of Fig. 1c at $T=0.27\text{K}$. The length of the samples was a) $0.3\mu\text{m}$, b) $0.5\mu\text{m}$, and c) $1\mu\text{m}$.

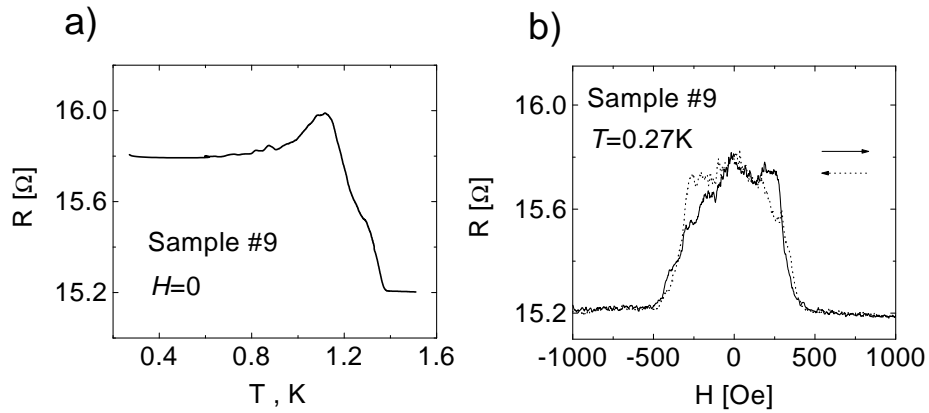


Fig. 6. Temperature dependence and magnetoresistance sample #9 of the geometry of Fig. 1c with length $L=1\mu\text{m}$.

Ferromagnetic Nanowires with Superconducting Electrodes

istics of three interfaces with different transparencies. We see a cross-over from negative to positive change in the resistance of the interface versus applied current upon increase of the interface resistance. The cross-over takes place at the specific interface resistance about $3 \times 10^{-9} \Omega \text{cm}^2$. Temperature dependencies reflect the same tendency.¹⁰

Figures 4 a) and b) show 3D applied current - magnetic field diagrams of samples # 3 and #5 respectively. There are a number of magnetic field independent peaks seen on these 3D diagrams. These peaks are small in amplitude but are clearly seen on all measured 3D diagrams of the contacts, including our best ones with interface resistance below 1Ω .

Proximity effect measured on samples with intermediate values of the interface transparency ($20 \Omega < R_b < 50 \Omega$) showed increase in the resistance upon the superconducting transition in the geometry of Fig. 1c. Figure 5 shows magnetoresistance of three samples of different length, L . All three show non-monotonic magnetoresistance with maxima in resistance at a magnetic field about 200 Oe. The final changes in the resistance, $R(H = 0) - R(H = 700 \text{Oe})$, are larger for longer samples.

Figure 6 shows temperature dependence and magnetoresistance curves for sample #9, geometry Fig. 1c. The temperature dependence shows a peak in resistance at the onset of superconductivity. The magnetoresistance curve shows a hysteresis in superconducting state similar to that of Fig. 2, but with opposite sign of resistance changes. The magnetoresistance of this structure above the transition showed the usual negative magnetoresistance of small ($\Delta R = 0.05 \Omega$) amplitude.

We have also studied the electron transport in the Andreev interferometer geometry of Fig. 1d. The magnetoresistance of the structure was measured with an accuracy down to $\Delta R/R^2 \sim 0.1 e^2/h$. In the first two samples tested, no phase-sensitive oscillations were detected so far.

4. DISCUSSION

Our experimental data confirms the existence of long-range effects in mesoscopic ferromagnet/superconductor structures, which was established in earlier works.^{7,8,9,10} The changes in conductance exceed greatly the value of e^2/h which excludes the mesoscopic origin of the effect observed. Such a giant amplitude of the changes in conductance is yet to be explained.

There were several attempts to account for the long-range superconducting proximity effect in ferromagnets. The authors of Ref. 11 suggest that due to spin-orbit interaction in the superconductor, the superconducting wave function may have a triplet component. The lifetime of the triplet state in the ferromagnet is much larger than that of a singlet one, therefore

this mechanism leads to the long-range effect. However, the estimate based on the formulas presented in Ref. 11 gives the values of the relative changes in conductance, $\Delta G/G$, more than 10^2 times smaller than the experimental values of few percent.

The contribution of the interface to the conductance of hybrid FS structures has been addressed theoretically in both ballistic^{5,12} and diffusive^{13,14,15} cases. The resistance of the diffusive FS interface was predicted to be always larger than that of the corresponding FN one. In contrast, in Fig. 3 we see a decrease in the resistance of the FS interface for samples with higher interface transparencies. For any interface transparency, we estimate the effect of the shunting by the small part of the superconductor to be of the order of or less than the resistance of one square of Al film. In our case it is 0.1 - 0.3 Ω . Since the changes in the resistance in Fig. 3 are considerably larger, we believe that shunting cannot explain the difference in behaviour.

The cross-over from positive changes in resistance to negative ones presented in Fig. 3 can be accounted for using the phenomenological analysis of Ref. 10. According to the latter the changes in the resistance of the ferromagnetic wire, $\Delta R_{FS} = R_{FN} - R_{FS}$, upon the superconducting transition can be written as:¹⁰

$$\frac{\Delta R_{FS}}{R_{FN}} = 1 - \frac{1}{\eta(1 - P(1 - \alpha))}, \quad (1)$$

where P is the spin polarization and η and α are phenomenological parameters. η is responsible for the conductance enhancement due to Andreev reflection and varies in the range $1 \leq \eta \leq 2$. Parameter α is proportional to the amount of the spin polarized current in proximity to the superconductor and varies in the range $0 \leq \alpha \leq 1$. Case $\alpha = 0$ corresponds to total spin filtering (no spin polarized current in the proximity of the ferromagnetic wire). While the Andreev reflections increase the conductance of the FS structure, the spin filtering decreases it. The competition between the two determines the final sign of the conductance changes. The two contributions may have different energy and magnetic field dependencies which may lead to non-monotonic dependencies like the ones presented in Fig. 5.

Magnetic field independent peaks on the dV/dI versus current, magnetic field 3D diagrams (Fig. 4), are present on all measurements of the structures in the geometry of Fig. 1b. The nature of the peaks is unclear.

The peak in resistance near the superconducting transition seen in Fig. 6a may be explained by the charge imbalance effect caused by the penetration of electric field into the superconductor.¹⁵ This resistance anomaly near the superconducting transition has been suggested to be a measure of the spin

Ferromagnetic Nanowires with Superconducting Electrodes

polarization of the ferromagnet¹⁵ and it requires additional experimental study.

The interesting feature of the presented data is the hysteresis in the magnetoresistance of the FS junctions. It is seen in Fig. 2 b) and c) and in Fig. 6 b). Note that the sign of the effect is opposite but hysteresis is present in both cases. This effect needs further investigation.

5. CONCLUSIONS

In conclusion, we have presented a systematic experimental study of mesoscopic ferromagnet/superconductor structures of various geometries. At the structures with high interface transparency we measured a giant long-range proximity effect. Values of the interface transparencies at which the cross-over from positive to negative changes in the resistance at the superconducting transition were found. Different theoretical approaches were discussed. While the theory can qualitatively explain the long-range superconducting proximity effect it fails to account for the amplitude of the effect. Further experimental and theoretical work is required.

ACKNOWLEDGMENTS

We thank C. Lambert, A. Volkov, A. Golubov, A. Zagoskin, and V. Chandrasekhar for useful discussions and A.F. Vyatkin for the SIMS analysis of the samples. We appreciate technical support from M. Venti. Financial support from EPSRC GR/L94611 is acknowledged.

REFERENCES

1. G.A. Prinz, *Physics Today* **48**, no. 4, 58 (1995).
2. R.J. Soulen *et al.*, *Science* **282**, 85 (1998).
3. S.K. Upadhyay, A. Palanisami, R.N. Louie, and R.A. Burman, *Phys. Rev. Lett.* **81**, 3247 (1998).
4. M.B. Stearns, *J. Magn. Magn. Mater.* **5**, 167 (1977).
5. M.J.M. de Jong and C.W.J. Beenakker, *Phys. Rev. Lett.* **74**, 1657 (1995).
6. E.A. Demler, G.B. Arnold, and M.R. Beasley, *Phys. rev. B* **55**, 15174 (1997).
7. V.T. Petrashov, V.N. Antonov, S. Maksimov, R. Shaikhaidarov, *JETP Lett.* **59**, 551 (1994).
8. M.D. Lawrence and N. Giordano, *J. Phys. Condens. Matter* **8**, L563 (1996).
9. M. Giroud, H. Courtois, K. Hasselbach, D. Mailly, and B. Pannetier, *Phys. Rev. B* **58**, 11872 (1998).
10. V.T. Petrashov, I.A. Sosnin, I.Cox, A. Parsons, C. Troadec, *Phys. Rev. Lett.*, **83**, 3281 (1999).
11. F. Zhou and B. Spivak, preprint, cond-mat/9906177.

V. T. Petrashov *et al.*

12. I. Zutic and O.T. Valls, preprint, cond-mat/9902080.
13. V.I. Falko, A.F. Volkov, C. Lambert, preprint, cond-mat/9901051.
14. F.J. Jedema, B.J. van Wees, B.H. Hoving, A.T. Filip, T.M. Klapwijk, preprint, cond-mat/9901323.
15. A.A. Golubov, preprint, cond-mat/9907194.